

# Target Specificity of an Autoreactive Pathogenic Human $\gamma\delta$ -T Cell Receptor in Myositis\*<sup>[5]</sup>

Received for publication, February 28, 2012. Published, JBC Papers in Press, May 1, 2012, DOI 10.1074/jbc.M112.356709

Jessica Bruder<sup>†§</sup>, Katherina Siewert<sup>†§</sup>, Birgit Obermeier<sup>†§</sup>, Joachim Malotka<sup>§</sup>, Peter Scheinert<sup>¶</sup>, Josef Kellermann<sup>||</sup>, Takuya Ueda<sup>\*\*</sup>, Reinhard Hohlfeld<sup>†§</sup>, and Klaus Dornmair<sup>†§1</sup>

From the <sup>†</sup>Institute of Clinical Neuroimmunology, Ludwig Maximilians University, D-81377 Munich, Germany, the <sup>§</sup>Department of Neuroimmunology, Max Planck Institute of Neurobiology, D-82152 Martinsried, Germany, <sup>¶</sup>AmpTec GmbH, Koenigstrasse 4a, D-22767 Hamburg, Germany, the <sup>||</sup>Department for Protein Analytics, Max Planck Institute of Biochemistry, D-82152 Martinsried, Germany, and the <sup>\*\*</sup>Department of Medical Genome Sciences, Graduate School of Frontier Sciences, The University of Tokyo, Building FSB-4015-1-5 Kashiwanoha, Kashiwa, Chiba Prefecture 277-8562, Japan

**Background:** In a rare case of human autoimmune myositis, muscle fibers are attacked by  $\gamma\delta$ -T cells.

**Results:** We identified several antigens recognized by the  $\gamma\delta$ -T cell receptor.

**Conclusion:** The  $\gamma\delta$ -T cell receptor recognized human tRNA synthetases known as antigens of autoantibodies in myositis.

**Significance:** This is the first report of an antigen recognized by human  $\gamma\delta$ -T cells in an autoimmune disease.

In polymyositis and inclusion body myositis, muscle fibers are surrounded and invaded by CD8-positive cytotoxic T cells expressing the  $\alpha\beta$ -T cell receptor ( $\alpha\beta$ -TCR) for antigen. In a rare variant of myositis, muscle fibers are similarly attacked by CD8-negative T cells expressing the  $\gamma\delta$ -TCR ( $\gamma\delta$ -T cell-mediated myositis). We investigated the antigen specificity of a human  $\gamma\delta$ -TCR previously identified in an autoimmune tissue lesion of  $\gamma\delta$ -T cell-mediated myositis. We show that this V $\gamma$ 1.3V $\delta$ 2-TCR, termed M88, recognizes various proteins from different species. Several of these proteins belong to the translational apparatus, including some bacterial and human aminoacyl-tRNA synthetases (AA-RS). Specifically, M88 recognizes histidyl-tRNA synthetase, an antigen known to be also targeted by autoantibodies called anti-Jo-1. The M88 target epitope is strictly conformational, independent of post-translational modification, and exposed on the surface of the respective antigenic protein. Extensive mutagenesis of the translation initiation factor-1 from *Escherichia coli* (EclF1), which served as a paradigm antigen with known structure, showed that a short  $\alpha$ -helical loop around amino acids 39 to 42 of EclF1 is a major part of the M88 epitope. Mutagenesis of M88 showed that the complementarity determining regions 3 of both  $\gamma\delta$ -TCR chains contribute to antigen recognition. M88 is the only known example of a molecularly characterized  $\gamma\delta$ -TCR expressed by autoaggressive T cells in tissue. The observation that AA-RS are targeted by a  $\gamma\delta$ -T cell and by autoantibodies reveals an unexpected link between T cell and antibody responses in autoimmune myositis.

wide range of physiological functions, they may also be involved in autoimmunity (5–7). A striking example of a putatively autoimmune human  $\gamma\delta$ -TCR<sup>2</sup> was described in 1991 (8). This  $\gamma\delta$ -TCR was isolated from muscle of a unique but well characterized patient with  $\gamma\delta$ -T cell-mediated myositis. In contrast to other forms of myositis where oligoclonally expanded CD8<sup>+</sup>  $\alpha\beta$ -T cells attack muscle fibers (9), in  $\gamma\delta$ -T cell-mediated myositis, muscle fibers are destroyed by monoclonally expanded T cells expressing a V $\gamma$ 1.3V $\delta$ 2<sup>+</sup>-TCR (8, 10). The monoclonal character of the T cell expansion allowed the cloning of both chains of this interesting  $\gamma\delta$ -TCR, subsequently referred to as M88.

To search for the target antigen(s), we expressed M88 on the surface of a T hybridoma cell line and as soluble single-chain Fv fragment excreted from COS-7 cells (11, 12). In earlier experiments, we found that presumably several target antigens may be recognized. All contain a protein component and a conformational rather than a linear epitope. Antigens were present in several species ranging from human muscle cells to bacteria. Moreover, we were unable to express M88 in the cytosol of any cell line, and we could not generate transgenic mice. Even bacteria stopped growing when M88 was induced in the cytosol. We therefore reasoned that M88 might bind to an intracellular proteinaceous motif that is essential for cell growth.

Here, we show that the target epitope of M88 is present on several structurally and functionally diverse proteins, including human and bacterial proteins of the translational apparatus. By extensive site-specific mutagenesis of a small paradigmatic protein, EclF-1, we obtained evidence that part of the epitope is exposed in a short  $\alpha$ -helix on the protein surface. Furthermore, we found that several aminoacyl-tRNA synthetases (AA-RS) were recognized. Although their structures are unknown, and they are quite large proteins, which impedes mutagenesis experiments, they are of particular interest because some of

$\gamma\delta$ -T cells are believed to act at the intersection between innate and adoptive immunity, and to be in the first line of defense against pathogens (1–4). Although  $\gamma\delta$ -T cells serve a

\* This work was supported by the Deutsche Forschungsgemeinschaft Grant SFB 571-A1 and the Hermann and Lilly Schilling Foundation.

<sup>[5]</sup> This article contains supplemental Table S1 and Figs. S1–S3.

<sup>1</sup> To whom correspondence should be addressed: Inst. of Clinical Neuroimmunology, Ludwig Maximilians University, D-81377 Munich, Germany. Tel.: 49-89-7095-4783; Fax: 49-89-7095-4782; E-mail: klaus.dornmair@med.uni-muenchen.de.

<sup>2</sup> The abbreviations used are: TCR, T cell receptor; AA-RS, aminoacyl-tRNA synthetases; EclF1, translation initiation factor-1 from *E. coli*; IMAC, immobilized metal affinity chromatography; hPCNA, human proliferating cell nuclear antigen; CDR, complementarity determining region.

these are known targets of autoantibodies in several forms of human myositis (13, 14). Although it is still unknown how the B cell responses to AA-RS evolve during pathogenesis, these autoantibodies are used as diagnostic markers of myositis. Our observation that AA-RS are targeted by autoaggressive  $\gamma\delta$ -T cells therefore reveals a surprising link between early, semi-innate immune responses mediated by  $\gamma\delta$ -T cells, and late responses mediated by mature, complement-activating autoantibodies.

## MATERIALS AND METHODS

**Screening of cDNA Libraries**—The host strain *E. coli* BL21-Star-DE3 (Invitrogen) was stably transfected with a described single chain Fv construct of our V $\gamma$ 1.3V $\delta$ 2<sup>+</sup>-TCR M88 (12) in the expression plasmid pET33b(+) (Novagene). The VN(D)NJ regions of the  $\gamma$ - and  $\delta$ -chains were connected by a 15-amino acid linker, but the construct used here did not contain a signal sequence. Bacteria were grown in the presence of 2 mM glucose and 50  $\mu$ g/ml kanamycin unless stated otherwise to suppress  $\gamma\delta$ -TCR expression. After washing the bacteria by centrifugation, they were resuspended in medium without glucose, and expression of M88 was induced by adding 2 mM isopropylthiogalactoside (Merck). Growth curves were recorded by determining the optical density of the bacterial suspension culture at 600 nm.

A cDNA expression library was constructed from mRNA of *E. coli* MG1655 (ATCC) and inserted into the expression plasmid pET21c(+) (Novagene). To this end, we first replaced the NdeI restriction site of pET21c(+) with a SmaI site by amplifying the sequence between the BglII and the NheI sites using the primer pair pET-BglII (5'-TAGAGGATCGAGATCTC-GATCC-3') and pET-Sma-Mut-rev (5'-AGTCATGCTAGC-CCCGGTATATCTCCTTC-3') and pET21c(+) as template for PCR. Then, the parent BglII-NheI fragment was replaced by the new fragment, which contained the replacement NdeI to SmaI. This plasmid was digested with SmaI and NotI, and the former insert was removed. In parallel, a cDNA expression library from *E. coli* MG1655 was established. Total RNA was extracted with TRIzol (Invitrogen) according to the manufacturer's instructions. Contaminating DNA was removed by DNase I treatment. *E. coli* mRNA was amplified using the ExpressArt Bacterial mRNA amplification kit (AmpTec), which yields amplified cDNA. In the final synthesis step, cDNA was synthesized according to the protocol for second round amplification with the exception that primer C was replaced by a primer that contained a NotI restriction site (5'-ATAGTT-TAgcgccgcGGGAGATTTTTTTTTTTT-3'. (The NotI site is underlined.) This product was finally digested with NotI. Due to the enzymes contained in the amplification kit, the library contains a blunt end on the other side. It was finally inserted into the plasmid pET21c(+) digested previously with SmaI and NotI.

M88-transfected *E. coli* BL21-Star-DE3 cells were supertransfected by electroporation at 2.5 kV, 200 ohm, 25  $\mu$ F in 2-mm electrode gap cuvettes with the cDNA library in pET21c(+) and grown for 30 min in LB medium with 2 mM glucose. Then ampicillin was added to a final concentration of 100  $\mu$ g/ml. After 30 min, kanamycin was added to a final con-

centration of 50  $\mu$ g/ml. After another 30 min, the bacteria were washed by centrifugation, resuspended in LB medium without glucose, and grown for a further 30 min. Then, expression was induced by adding isopropylthiogalactoside to a final concentration of 1 mM. After 30 min, bacteria were grown on agar plates that contained 100  $\mu$ g/ml ampicillin, 50  $\mu$ g/ml kanamycin, and 1 mM isopropyl thiogalactoside. After incubation for 40 h at 37 °C, the biggest colonies were picked and grown in suspension cultures in the presence of ampicillin and glucose, and plasmids were prepared and sequenced by standard methods. As a control experiment, we plated the bacteria on plates that contained 1% glucose, 100  $\mu$ g/ml ampicillin, 50  $\mu$ g/ml kanamycin, but without isopropyl thiogalactoside to shut down the promoter. Colonies of similar size became visible already after 18 h at 37 °C.

**Peptides, Proteins, and Antibodies**—The synthetic peptide EcIF1(33–46), which represents amino acids 33–46 of EcIF1, was synthesized by solid phase peptide synthesis and purified by reversed phase HPLC. Its correct sequence was verified by mass spectrometry. The purified recombinant human proteins His-, Thr-, and Ala-tRNA synthetases hH-RS (Jo-1), hT-RS (PL-7), hA-RS (PL-12), human formimidoyltransferase-cyclo-deaminase (hLC1) and human proliferating cell nuclear antigen (hPCNA) were purchased from Diarect (Freiburg). All human proteins were produced identically in a baculovirus expression system and purified by immobilized metal affinity chromatography (IMAC). The polyclonal anti-Jo-1 human Ig fraction BP2040 was purchased from Acris, the monoclonal mouse  $\alpha$ -Jo-1 IgG1 antibody HARSA6 was from GenWay, and the isotype control monoclonal mouse IgG1 Pure antibody X40 was from BD Biosciences. The anti-mouse CD3 $\epsilon$  antibody 145–2C11 (BD Biosciences) was used as control for  $\gamma\delta$ -TCR activation. All bacterial proteins are contained in the PUREexpress *in vitro* translation kit (New England Biolabs). They were expressed in the cytosol of *E. coli* and purified by IMAC as described (15). In contrast to the kit, where the proteins are pooled, here, all proteins were expressed and tested individually.

**Cloning, Expression, and Purification of Wild-type and Mutated EcIF1**—Total RNA from *E. coli* SG13009 (Qiagen) was isolated using the RNeasy mini kit and RNase-free DNase Set (Qiagen). cDNA was prepared using the clone-specific primer IF1wt-rev and SuperScript III reverse transcriptase (Invitrogen). *E. coli* IF1 wild-type cDNA was amplified using the primers IF1wt-for and IF1wt-rev. See supplemental Table S1 for all primer sequences. The PCR reaction was carried out for 40 cycles at 94 °C, 56 °C, and 72 °C for 1 min each. The PCR product was cloned into pCR2.1. TOPO (Invitrogen), which served as a template for all further experiments.

Site-directed mutagenesis was performed using a PCR-based method: nucleotides coding for the amino acid of choice were introduced into forward (Mut-for) and reverse (Mut-rev) PCR primers (supplemental Table S1) that span the selected positions. In addition, these primers contained silent nucleotide exchanges to introduce unique restriction sites at positions that closely flanked the desired mutation. Two fragments were amplified. For the first fragment we used the primer IF1-wt-for-BamHI together with one of the reverse primers IF-X-rev-Y,

## Targets of an Autoreactive Human $\gamma\delta$ -TCR

where X denoted the amino acid to be exchanged, and Y denoted the restriction site to be inserted. For the second fragment, we used the primer IF1-wt-rev-HindIII together with one of the forward primers IF-X-for-Y. The conditions of the PCR reactions were as described above. The PCR fragments were digested with the restriction enzymes Y, purified, and ligated, and a second PCR was performed using primers IF1wt-for-BamHI and IF1wt-rev-HindIII only.

The PCR products encoding the full-length sequences of IF1 wild-type and mutants were cloned into the plasmid pCR2.1-TOPO, digested with the restriction enzymes BamHI and HindIII and cloned into the BamHI and HindIII sites of expression plasmid pQE30 (Qiagen), which carries a sequence coding for a His<sub>6</sub> tag at the N terminus. Therefore, the expressed proteins are extended for the N-terminal sequence, MRGS-His<sub>6</sub>-GS. Plasmids were transfected into *E. coli* strain DH5 $\alpha$ -F'IQ (Invitrogen). As negative control, we used *E. coli* DH5 $\alpha$ -F'IQ transfected with myelin oligodendrocyte glycoprotein (16). Bacteria were grown in LB containing 100  $\mu$ g/ml ampicillin (Sigma). Protein expression was induced at a cell density of 0.4–0.5  $A_{600\text{ nm}}$  by adding isopropylthiogalactoside to a final concentration of 2 mM. Bacteria were harvested after 4 h by centrifugation for 5 min at 15,000  $\times g$ .

Bacterial pellets from a 250-ml culture were resuspended in 70 ml of lysis buffer (50 mM sodium phosphate buffer, 300 mM NaCl, 10 mM imidazole, 0.05 mg/ml DNase (Sigma) 10 mM MgCl<sub>2</sub>, 5  $\mu$ g/ml aprotinin (Sigma), 0.1 mM PMSF, 1 mg/ml lysozyme (Sigma), pH 8.0) and lysed by sonication on ice for 15 min at 30 W using a Branson 450 sonifier. After centrifugation for 10 min at 15,000  $\times g$  the supernatants were purified by IMAC. The supernatants were loaded at a flow rate of 1 ml/min onto 5-ml nickel-nitrilotriacetic acid-agarose columns (Qiagen) equilibrated with lysis buffer. The columns were washed with 10–15 column volumes of 50 mM sodium phosphate buffer, 300 mM NaCl, 50 mM imidazole, pH 8.0, and eluted with 50 mM sodium phosphate buffer, 300 mM NaCl, 250 mM imidazole, pH 8.0. Purified proteins were dialyzed against 10 mM sodium phosphate buffer (pH 7.4), 150 mM NaCl, or 50 mM sodium phosphate buffer, 300 mM NaCl, pH 7.8, and stored at  $-80^\circ\text{C}$ . Bacteria expressing myelin oligodendrocyte glycoprotein were treated identically. Because this protein precipitates quantitatively in inclusion bodies, this mock preparation contains only co-purifying contaminating bacterial proteins.

**Analytical Procedures and Size Exclusion HPLC**—Protein concentrations were measured according to Peterson *et al.* (17). Purity of the proteins was assessed by SDS-PAGE using 4–20% tris-glycine polyacrylamid Novex protein gels (Invitrogen). Gels were stained by Coomassie Blue (Fluka) or with silver (18).

We confirmed the native secondary structure of EcIF1 by measuring circular dichroism spectra at 25  $^\circ\text{C}$  in the range from 195 to 250 nm using a Jasco J-715 spectrometer. The protein concentration was 18.3  $\mu\text{M}$  in 10 mM sodium phosphate buffer, pH 7.4, 150 mM NaCl. The spectrum of the buffer was subtracted prior to data analysis. The experimental curves were fitted to a set of standard proteins using the program Spectra Manager CDProAnalysis Contin SMP56 (Jasco).

For some experiments, proteins were further purified by size exclusion chromatography. We used a 7.8 mm  $\times$  30 cm TSK-

Gel G2000SWXL 5–150 kDa column with a particle size of 5.0  $\mu\text{m}$  (Tosoh Bioscience) and HP1100 HPLC equipment (Agilent). Chromatography was performed in 200 mM sodium phosphate buffer, 200 mM NaCl, pH 6.8, at a flow rate of 0.8 ml/min. 27–30  $\mu\text{g}$  of protein were injected, and >12 fractions in a time range of 5–21 min were collected.

**Cloning, Expression, and Activation of Wild-type and Mutated  $\gamma\delta$ -TCR Molecules**—The cDNAs of M88 wild-type chains and chains carrying a set of mutated  $\gamma$ - and  $\delta$ -chains with altered V-, N(D)N(J)-, or C $\gamma$ - regions were cloned into expression plasmids, and expressed on the surface of the T hybridoma cell line 58 $\alpha^- \beta^-$  (19), which lacks endogenous TCR chains, as described (11, 12). 58 $\alpha^- \beta^-$  cells express the CD3 complex and the downstream signaling machinery for secreting mouse interleukin-2 (IL-2) after TCR activation by antigens. Individual clones were picked and analyzed independently. All selected clones expressed the heterodimeric  $\gamma\delta$ -TCR on their surface and were capable of IL-2 secretion after TCR activation by antigens.

For all T cell activation experiments, the candidate and control proteins were coated to flat-bottomed 96-well tissue culture plates (Costar). EcK-RS and the anti-CD3 $\epsilon$  control antibody 145-2C11 were coated for 3 h at 37  $^\circ\text{C}$  at 20  $\mu\text{g}/\text{ml}$  and 1  $\mu\text{g}/\text{ml}$ , respectively, in 10 mM sodium phosphate buffer, pH 7.4, 150 mM NaCl. Samples from the HPLC columns were coated directly in HPLC buffer and incubated for 3 h at 37  $^\circ\text{C}$ . For testing antigen recognition of wild-type M88-transfectants or mutants with altered TCR  $\gamma$ - or  $\delta$ -chains, 10  $\mu\text{g}/\text{well}$  wild-type EcIF1 was coated for 3 h at 37  $^\circ\text{C}$ .

To detect direct M88 activation by human recombinant proteins and for the antibody blocking assay, the candidate proteins were coated at 0.5  $\mu\text{g}/\text{well}$  in 50  $\mu\text{l}$  of 10 mM sodium phosphate buffer, 150 mM NaCl, pH 7.4, for 2 h at 37  $^\circ\text{C}$ . Then, the plates were washed with buffer. For the antibody blocking assay, 50  $\mu\text{l}$  of antibody solution in RPMI 1640 medium (Invitrogen) supplemented with 5 to 10% heat-inactivated fetal bovine serum (lot 075K3398 (Sigma)), 1.5 mg/ml geneticin (Invitrogen) and 0.3 mg/ml hygromycin B (Invitrogen) were incubated for 30 min at 37  $^\circ\text{C}$  with the coated candidate proteins. The polyclonal anti-Jo-1 human Ig fraction BP2040 was used at dilutions of 1:10 and 1:100, and the monoclonal mouse  $\alpha$ -Jo-1 IgG1 antibody HARSA6 at 10  $\mu\text{g}/\text{ml}$  final concentration. The monoclonal mouse IgG1 Pure antibody X40 served as isotype control at 10  $\mu\text{g}/\text{ml}$ .

To test recognition of the synthetic peptide EcIF1(33–46), it was coated at concentrations between  $5.0 \times 10^2$  and  $5.0 \times 10^{-5}$   $\mu\text{g}/\text{well}$  for 3 h at 37  $^\circ\text{C}$  in 10 mM sodium phosphate buffer, pH 7.4, 150 mM NaCl. To test competition of EcIF1(33–46) with wild-type EcIF1, EcIF1 was coated at 0.5  $\mu\text{g}/\text{well}$  for 3 h at 37  $^\circ\text{C}$  in 10 mM sodium phosphate buffer, pH 7.4, 150 mM NaCl. After washing the wells with buffer, EcIF1(33–46) was added at concentrations between 666.0 and  $3.3 \times 10^{-4}$   $\mu\text{g}/\text{ml}$  together with M88 transfected hybridoma cells.

For investigating recognition of denatured EcIF1, recombinant EcIF1 was coated at 0.5  $\mu\text{g}/\text{well}$  for 3 h at 37  $^\circ\text{C}$  in 10 mM sodium phosphate buffer, pH 7.4, 150 mM NaCl. Then, the wells were washed with buffer, and the samples were incubated for 24 h at 37  $^\circ\text{C}$  with 6 M guanidinium thiocyanate, 2 M HCl, 5 M



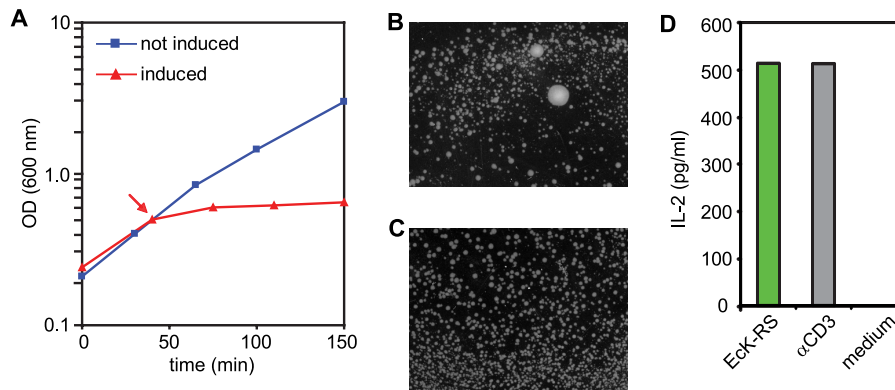


**FIGURE 1. Screening of a cDNA library.** *A*, growth curves of *E. coli* BL21-Star-DE3 cells transfected with the single-chain Fv  $\gamma\delta$ -TCR M88. Blue line and squares: bacterial growth in the absence of M88 expression. Red line and triangles, growth with induction of M88 expression. The time point of induction by isopropylthiogalactoside is indicated by an arrow. After induction of M88, bacterial growth was drastically inhibited. *B*, bacteria expressing the single-chain Fv M88 are rescued from its growth inhibitory effect by supertransfection with a cDNA library. Some components of the library rescued the bacteria, presumably by binding to and neutralizing M88. This yielded big colonies from which the inserts of the library could be cloned and sequenced. Many small colonies were observed in addition, in which the library components did not neutralize the growth-inhibiting effect of M88. *C*, control experiments in which the promoter driving M88 expression was shut down in the presence of 2 mM glucose. All colonies were of approximately the same size. To prevent formation of a confluent layer of bacteria, colonies were grown for a shorter period of time. *D*, activation of M88 by Eck-RS. Eck-RS was identified as one of the cDNA library components that could rescue M88-transfected *E. coli* BL21-Star-DE3. We tested recognition of purified Eck-RS in an ELISA experiment. Eck-RS and an anti-CD3 antibody ( $\alpha$ -CD3-mAb) as positive control were coated to microtiter plates, M88-transfected T hybridoma cells were added, and secreted IL-2 was measured in the supernatant. Eck-RS and the  $\alpha$ -CD3-mAb both activated M88, whereas medium alone had no effect.

NaOH, or 200  $\mu$ g/ml proteinase K (Roche). EcIF1 was digested in solution with 1  $\mu$ g/ml trypsin (Merck) in 25 mM Tris/HCl buffer, pH 8.5, for 3 h at 37  $^{\circ}$ C and coated thereafter.

For the dose-response experiments, EcIF1 wild-type and mutant proteins were centrifuged before use in 30-kDa spin columns (Amicon, Millipore) for 20 min at 3,000  $\times$  *g*. After centrifugation, the protein concentration of the flow-through was measured. Proteins were coated at concentrations between 0.1 and 10  $\mu$ g/well in 50  $\mu$ l of 50 mM sodium phosphate buffer, 300 mM NaCl, pH 7.8, for 3 h at 37  $^{\circ}$ C.

For all experiments, the coated plates were washed with RPMI 1640 medium (Invitrogen), except for the antibody-blocking experiments, where the plates were not washed. Then, 40,000 M88 transfectants were added to each well at a final volume of 150  $\mu$ l in medium as described above and incubated for 17 h at 37  $^{\circ}$ C in a 5% CO<sub>2</sub> atmosphere. Finally, 50  $\mu$ l of supernatant were removed, and mouse IL-2 was measured by ELISA (eBioscience). Background signals from samples without antigens were subtracted, and absolute IL-2 concentrations were determined using a standard curve.

## RESULTS

**Hints from cDNA Library Screening**—As an initial step toward identification of the target antigen of the  $\gamma\delta$ -TCR M88, we “rescued” *E. coli* cells from the growth-inhibiting effects of M88 by supertransfecting the bacteria with a cDNA library. Growth of bacteria was halted when the expression of a single-chain Fv construct (12) of M88 was induced in the cytosol of *E. coli* BL21 (Fig. 1A). Because there were no reasons to assume that M88 was toxic (the protein is not particularly hydrophobic or charged and presumably has no enzymatic activity), we surmised that M88 might bind and neutralize a bacterial compound that is essential for cell growth. We further knew from previous experiments that a protein moiety is at least part of the antigen (11). Therefore, we supertransfected M88-expressing bacteria with a cDNA library from *E. coli* to rescue them from

growth inhibition by M88. Clones expressing library coded proteins that contain the antigen would be expected to bind to M88 and neutralize it. Such bacteria would grow in big colonies, whereas clones that contain irrelevant transcripts would yield small colonies or would not grow at all. Indeed, after supertransfection with the Fv-M88 and the library and induction of M88 and library expression, we observed many very small bacterial clones but also a few clones that grew to very big colonies (Fig. 1B). Under conditions where M88 expression was prevented, all colonies were of the same size (Fig. 1C). We picked some of the biggest colonies and sequenced the inserts of the plasmids coding for the library. In two clones, we identified *E. coli* lysyl-tRNA synthetase (Eck-RS) as a candidate antigen. To confirm that Eck-RS contains the antigenic epitope, we coated purified, recombinant Eck-RS (15) to a microtiter plate, added T hybridoma cells that expressed M88 (11), and measured secreted IL-2 in the supernatant. We found that M88 indeed recognizes Eck-RS (Fig. 1D).

**$\gamma\delta$ -TCR M88 Recognizes Several Bacterial Proteins**—Because we surmised that M88 might recognize an epitope present on several proteins, we tested other proteins from the translation apparatus of *E. coli* (15). Several proteins were indeed recognized. Although all proteins were highly purified, some minor contaminations were detectable in some of the preparations (supplemental Fig. S1A). To exclude that such contaminations were recognized, we subjected some of the samples to size-exclusion HPLC and tested all eluted fractions for M88-activating capacity (Fig. 2). We found that in addition to Eck-RS, the *E. coli* AA-RS for asparagine (EcN-RS) and the EcIF1 1 (*E. coli* translation initiation factor) specifically activated M88 because M88 activation was observed only with fractions that contained the respective proteins. By contrast, AA-RS for aspartic acid (EcD-RS) was not recognized (Fig. 2). Together, these data show that M88 recognizes several functionally and structurally different bacterial proteins.

## Targets of an Autoreactive Human $\gamma\delta$ -TCR

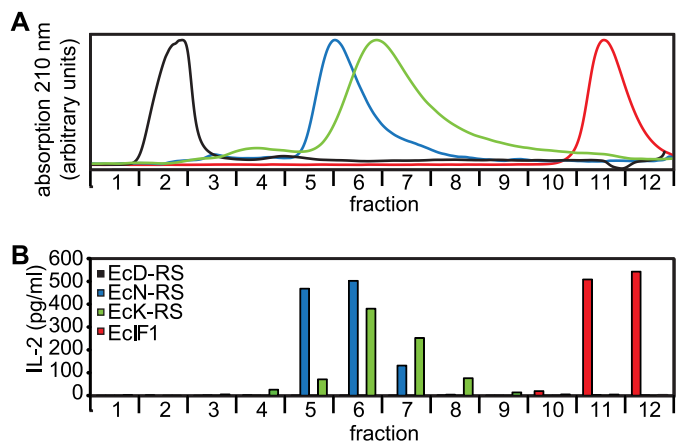


**FIGURE 2. Recognition of diverse bacterial proteins.** *A*, size-exclusion HPLC chromatography of the recombinant *E. coli* proteins EcK-RS (green curve), EcD-RS (black curve), EcN-RS (blue curve), and EcIF1 (red curve). All proteins were produced identically in *E. coli*. Elution profiles were recorded at 210 nm. 12 fractions were collected in the range from 150 to 5 kDa. Purity of all proteins was tested by SDS-PAGE before and after chromatography (supplemental Fig. S1A). EcD-RS migrated faster than expected, presumably because it formed oligomers. *B*, activation of M88 transfectants by the HPLC fractions shown in *A*. All fractions from all proteins were coated to microtiter plates and tested for their capability to activate M88 transfectants. To this end, we measured secreted IL-2 in the supernatant. The color coding is identical to that described in *A*. Activation of M88 transfectants was coincident with the elution peaks for EcK-RS, EcN-RS, and EcIF1. EcD-RS did not activate M88.

**$\gamma\delta$ -TCR M88 Recognizes Several Human Proteins**—Because we knew that M88 may also recognize proteins from human muscle cell extracts (11), we tested recombinant human AA-RS for histidine and alanine (hH-RS, hA-RS), which are also known as myositis antigens “Jo-1” and “PL-12”. As above, we performed size-exclusion HPLC to exclude that contaminations were recognized (Fig. 3 and supplemental Fig. S1B). M88 activation was observed only in fractions containing hH-RS and hA-RS, providing evidence that these proteins were recognized directly. M88 activation was not limited to AA-RS because also hLC1 (20), a hepatitis antigen, was recognized. The control protein hPCNA, which was identically produced and purified, was not recognized.

Activation of hH-RS was specific, as it was blocked completely by a polyclonal anti-serum and by a monoclonal antibody against hH-RS (Fig. 4). Recognition of hA-RS and of the human AA-RS for threonine (hT-RS, synonym PL-7) could also be blocked by high concentrations of the polyclonal anti-serum but not by the monoclonal antibody. Thus, we showed by two independent experiments that hH-RS was recognized specifically. Furthermore, as expected, also other unrelated human proteins activated M88.

**Characterization of M88 Target Epitope by Site-directed Mutagenesis**—To characterize the epitope, we used the small soluble protein EcIF1 as a paradigm. EcIF1 is composed of only 72 amino acids and carries no post-translational modifications. Its structure is known (Fig. 5A) (21), in contrast to the human AA-RS molecules, where no structural information of the complete proteins is available. EcIF1 was expressed in *E. coli* and purified to homogeneity. It is known that wild-type EcIF1 expressed by this method is functional (15), and we further

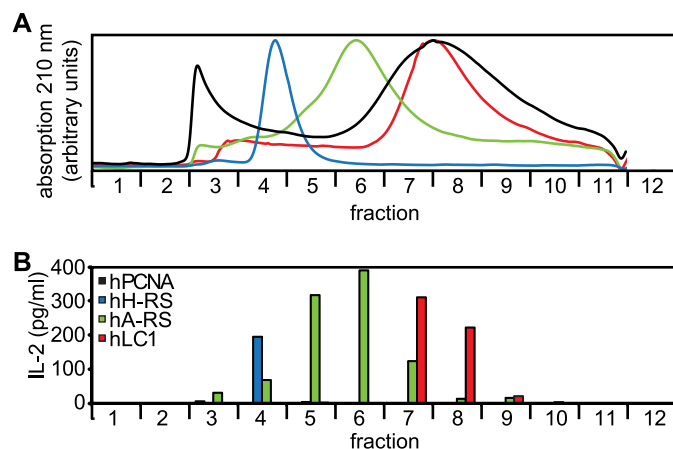


**FIGURE 3. Recognition of diverse human proteins.** *A*, size-exclusion HPLC chromatography of the recombinant human proteins hH-RS (blue curve), hA-RS (green curve), hLC1 (red curve), and hPCNA (black curve). All proteins were produced identically in insect cells. Purity of all proteins was tested by SDS-PAGE before and after chromatography (supplemental Fig. S1B). hH-RS migrated with a higher molecular mass than expected, indicating oligomerization. hA-RS and hLC1 were retained presumably due to interaction with the column matrix. hT-RS denatured during chromatography and could not be detected in the eluate (data not shown). *B*, size-exclusion HPLC chromatography of the recombinant human proteins shown in *A*. IL-2 production was measured as detailed in Fig. 2B. Activation of M88 transfectants was coincident with the elution peaks for hH-RS, hA-RS, and hLC1. hPCNA was not recognized. Data represent two independent experiments.

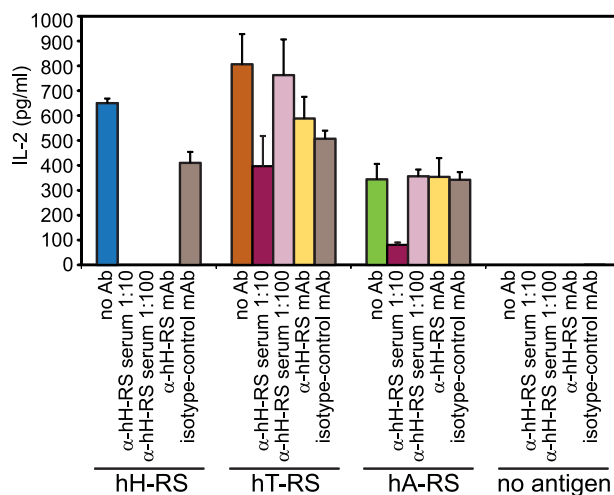


**FIGURE 4. Specific recognition of human aminoacyl-tRNA-synthetases by M88.** The putative antigens hH-RS (blue bar), hT-RS (orange bar), and hA-RS (green bar) were tested for activation of M88. Candidate antigens were coated to microtiter plates, incubated with M88-transfected T hybridoma cells in the absence or presence of blocking antibodies, and secreted IL-2 was measured in the supernatant. Recognition of hH-RS by M88 could be blocked by two types of specific antibodies (Ab). We used polyclonal human serum ( $\alpha$ -hH-RS serum) at two different dilutions (1:10 and 1:100, dark and light red bars, respectively), and a monoclonal antibody ( $\alpha$ -hH-RS mAb, yellow bar). The isotype control antibody X40 (isotype control mAb, gray bar) did not block recognition. Recognition of hT-RS and hA-RS could only be blocked at the high concentration of polyclonal  $\alpha$ -hH-RS serum, indicating some cross-reactivity. Recognition of hA-RS was lower than recognition of hH-RS or hT-RS. This may be explained by the presence of more contaminating proteins (supplemental Fig. S1B) that may compete for binding to the microtiter plate. However, M88 activation could also be blocked to some extent by high concentrations of  $\alpha$ -hH-RS serum. The antibodies alone did not induce IL-2 secretion. Error bars represent  $\pm$  S.E. Data represent four independent experiments.

show here by circular dichroism spectroscopy that the purified EcIF1 adopts a native secondary structure (supplemental Fig. S2).

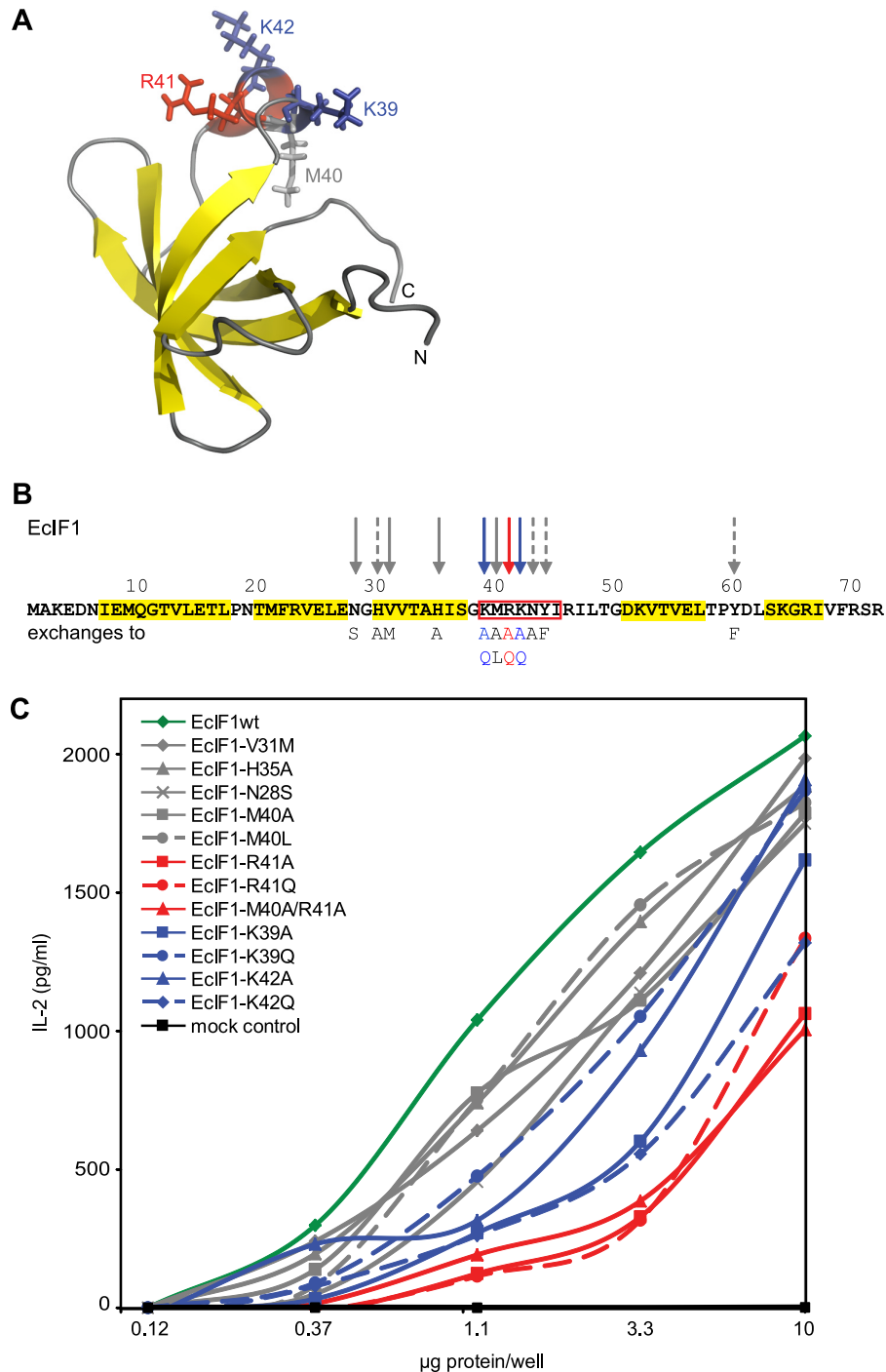


**FIGURE 5. Amino acids of the target antigen EclF1 recognized by M88.** *A*, structural model of EclF1 based on NMR spectroscopy (21). The entire molecule is shown in ribbon presentation. The five  $\beta$ -sheets that form a rigid  $\beta$ -barrel are shown in yellow. The amino acids Lys-39 (blue), Met-40 (gray), Arg-41 (red), and Lys-42 (blue) in the short helix, which is recognized by the  $\gamma\delta$ -TCR, are highlighted as stick models. We used Protein Data Bank code 1AH9 (no.11) and the program PyMOL for display. *B*, amino acid sequence of EclF1 of *E. coli*. The structural elements shown in *A* are indicated:  $\beta$ -sheets are highlighted in yellow, and the  $\alpha$ -helix is boxed in red. The 15 amino acids that were exchanged by site-directed mutagenesis are indicated by arrows. The most relevant amino acid, Arg-41, is indicated by a red arrow. The two other relevant amino acids, Lys-39 and Lys-42, are indicated by blue arrows. Other amino acids are indicated by gray arrows. Continuous arrows indicate amino acid exchanges where the data are shown in *C* (Asn-28, Val-31, His-35, Met-40). Dashed gray arrows indicate amino acids that were tested but without showing the data in *C* (His-30, Asn-43, Tyr-44, Tyr-60). *C*, activation of M88 transfectants by EclF1 wild-type protein and by EclF1 molecules carrying site-specific mutations. M88 transfectants were incubated with wild-type and mutated EclF1 proteins, which were coated to microtiter plates at the indicated concentrations. TCR activation was determined by measuring the secreted IL-2 in the supernatant. EclF1 wild-type data are shown in dark green. The color code for the different amino acid substitutions is given in the inset. It is identical to the color code used in *B*. Amino acid substitutions that are indicated with dashed gray arrows in *B* were also tested but are not shown here. They all showed no significant deviation from the data of the wild-type. We also include a mock control, i.e. bacteria that expressed myelin oligodendrocyte glycoprotein, which forms insoluble inclusion bodies. An identically prepared sample from these bacteria contains all bacterial contaminations. It did not activate M88 (black squares). Data were statistically significant with  $p$  values of  $< 0.05$  according to a Student's two-tailed unpaired  $t$  test at protein concentrations of 1.1, 3.3, and 10  $\mu\text{g/well}$  for the mutants R41A, R41Q, M40A/R41A, K42Q, and K39A, respectively. Data represent four independent experiments.



## Targets of an Autoreactive Human $\gamma\delta$ -TCR

We probed the surface of EclF1 for immunogenic regions by introducing 16 site-specific mutations (Fig. 5B). Wild-type and mutated proteins were expressed in *E. coli*, purified to homogeneity (supplemental Fig. S3), and M88 activation was measured (Fig. 5C). Only exchanges of the positively charged amino acids around position 40 (Fig. 5B) had significant effects. This short  $3_{10}$   $\alpha$ -helix is located in a loop that reaches out from the core of the protein (Fig. 5A). Other substitutions showed only minor differences to the wild-type EclF1. We exchanged Lys-39, Met-40, Arg-41, and Lys-42 individually to alanine and to structurally related amino acids, *i.e.* Lys to Gln, Met to Leu, and Arg to Gln (Fig. 5B). We found that exchanges Arg-41 to Ala or Gln significantly decreased recognition. Met-40 is presumably irrelevant because it points to the opposite side of the epitope (Fig. 5A). Substitutions of Lys-39 and Lys-42 showed surprising effects: the exchange K39A diminished recognition, whereas K39Q was recognized like the wild-type, indicating that the aliphatic carbon atoms C3 and/or C4 are required. The substitution K42A activated better than K42Q. The bulky side chain may thus impose a sterical hindrance, which may be compensated by introduction of a positive charge. These substitutions show that Lys-39, Arg-41, and Lys-42 are part of the epitope recognized by M88 but that the positive charges *per se* are not absolutely required. Furthermore, the mutagenesis experiments show that amino acids are recognized directly, excluding that post-translational modifications or non-covalently bound ligands are involved.

We confirmed that the surface-exposed epitope is not linear but rather conformational because a peptide representing amino acids 33 to 46 (EclF1(33–46)) was not recognized directly by M88 (Fig. 6A), and EclF1(33–46) was not able to compete with the correctly folded EclF1 for M88 binding (Fig. 6B). Furthermore, denaturation of EclF1 by acid or base treatment, unfolding of EclF1 secondary structure by the chaotropic agent guanidinium thiocyanate, or destruction of the epitope by protease digestion, all abrogated EclF1 recognition (Fig. 6C).

**Specific Antigen Recognition through Complementarity Determining Regions of M88**—To show that EclF1 was recognized specifically by the complementarity determining regions (CDR) of M88, we employed  $\gamma\delta$ -TCR molecules with exchanged variable regions or with defined amino acid exchanges in the CDR3 loops of either chain (11, 12). All exchanges, including replacement of only few amino acids in the CDR3 loops of both chains, abolished recognition completely (Fig. 7), whereas exchange of the conserved region of the  $\gamma$ -chain showed no effect. This provides evidence that M88 recognizes EclF1 specifically with its CDR loops and uses both chains for antigen binding, although it remains open whether each of the six CDR loops contributes equally significantly. This is similar to a prenyl-pyrophosphate-specific  $\gamma\delta$ -TCR (22) but different from  $\gamma\delta$ -TCRs that bind non-classical MHC molecules only by their CDR3 $\delta$  loop (23).

## DISCUSSION

We investigated the target specificity of the autoreactive human  $\gamma\delta$ -TCR M88 that was initially isolated from muscle lesions of a patient with autoimmune  $\gamma\delta$  T cell-mediated myositis (8, 10). We expressed M88 on the surface of a T hybridoma

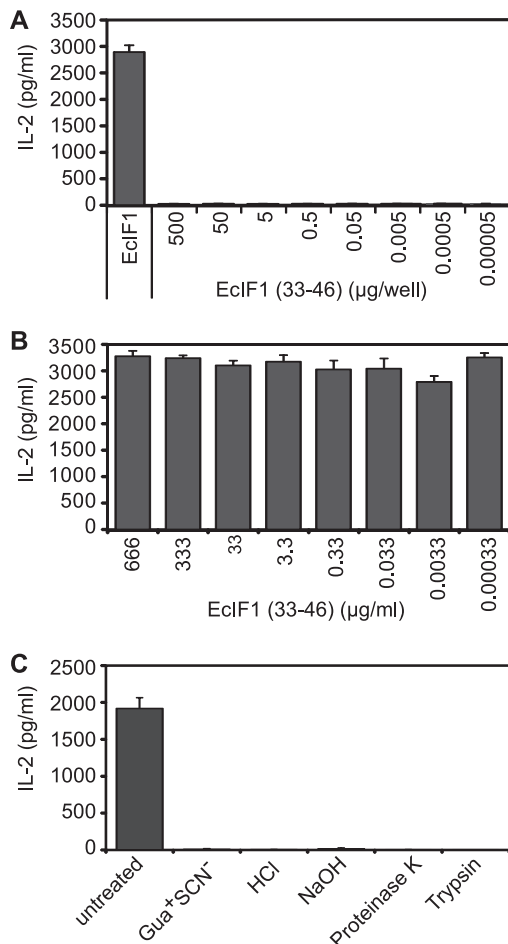


**FIGURE 6. M88 recognizes a conformational epitope.** A, the synthetic peptide EclF1(33–46) did not activate M88 when coated to microtiter plate wells at concentrations between  $5.0 \times 10^2$  and  $5.0 \times 10^{-5}$   $\mu\text{g}/\text{well}$ . Wild-type EclF1 in its native conformation was coated at  $0.5$   $\mu\text{g}/\text{well}$  and served as positive control (*left panel*). B, EclF1(33–46) did not compete with wild-type EclF1 for activation of M88. EclF1 was coated at  $0.5$   $\mu\text{g}/\text{well}$  to microtiter plates, plates were washed, and then EclF1(33–46) was added at concentrations between  $6.6 \times 10^2$  and  $3.3 \times 10^{-4}$   $\mu\text{g}/\text{ml}$  together with M88-transfected hybridoma cells. Recognition of EclF1 was not influenced by the synthetic peptide EclF1(33–46). C, wild-type EclF1 was denatured by exposure to  $6$  M guanidinium thiocyanate ( $\text{Gua}^+ \text{SCN}^-$ ),  $2$  M HCl,  $5$  M NaOH. Furthermore, EclF1 was subjected to digestion with the proteases proteinase K and trypsin. All conditions abolished recognition by M88. We show untreated wild-type EclF1 as positive control experiment. Error bars represent  $\pm$  S.E.

cell line and as soluble single-chain Fv fragment and used these constructs for preliminary antigen searches (11, 12). Hints from cDNA library screening experiments helped us to identify several proteins that were able to stimulate M88. Extensive mutagenesis of a paradigmatic protein allowed us to identify several distinct features of the target antigen(s). Specifically, our results suggest that the target epitope of M88 is (a) present on, but not exclusive to, several proteins of the translational apparatus including several human AA-RS; (b) strictly conformational; (c) independent of post-translational modification; (d) exposed on the protein surface; (e) partly represented by the short  $\alpha$ -helical loop of region 39–42 of EclF1; and (f) contacted by the CDR3 regions of both the  $\gamma$ - and  $\delta$ -chain of M88.

So far, only very few  $\gamma\delta$ -TCR epitopes have been resolved at the molecular level (1–4).  $\gamma\delta$ -T cells recognize their antigens, like antibodies, in an MHC-non-restricted way, but, similar to

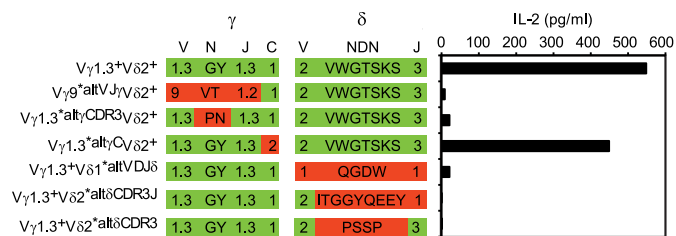


**FIGURE 7. Specific recognition of the paradigmatic antigen EclF1 by the CDR loops of the  $\gamma\delta$ -TCR.** We compared the recognition of EclF1 by the wild-type M88 and M88 molecules that contained mutations in the variable (V) and/or CDR3 regions of either chain. CDR3 regions are composed of random nucleotides (N), diversity (D), and joining (J) elements. The first row lists the wild-type  $\gamma\delta$ -TCR M88 ( $V\gamma 1.3^+V\delta 2^+$ ), and the TCR transfectants with mutated  $\gamma$ - or  $\delta$ -chains: two mutants had altered V(D)J regions of either chain ( $V\gamma 9^{\text{altVJ}}V\delta 2^+$ ,  $V\gamma 1.3^+V\delta 1^{\text{altVDJ}\delta}$ ), three mutants had amino acid exchanges in the  $\gamma$ -N region ( $V\gamma 1.3^{\text{altV}}\text{CDR3}V\delta 2^+$ ), the  $\delta$ -NDN ( $V\gamma 1.3^+V\delta 2^{\text{alt}\delta}\text{CDR3}$ ), or  $\delta$ -NDNJ regions ( $V\gamma 1.3^+V\delta 2^{\text{alt}\delta}\text{CDR3J}$ ), and one mutant had wild-type V(D)J regions, but an altered constant region (C) of the  $\gamma$ -chain ( $V\gamma 1.3^{\text{altV}}V\delta 2^+$ ). The second and third rows illustrate these exchanges. We list the variable and joining families of the  $\gamma$ - and  $\delta$ -chains (V-region nomenclature according to Arden *et al.* (50)), and show the amino acids of the N- or NDN regions in the single amino acid code. Wild-type regions and amino acids are highlighted in green, and exchanges of entire regions or amino acids are highlighted in red. On the right panel, we show the activation of  $\gamma\delta$ -TCR transfectants by EclF1. EclF1 was adsorbed to microtiter plates, incubated with  $\gamma\delta$ -TCR transfected hybridoma cells, and secreted IL-2 was measured by ELISA. Only the wild-type  $V\gamma 1.3V\delta 2$ -TCR M88 and the mutant with altered  $\gamma$ -chain constant region recognized EclF1. All other mutants with altered V- and/or CDR3 regions were not activated. This provides evidence that EclF1 is recognized specifically by the complementarity determining regions. Data represent two independent experiments.

$\alpha\beta$ -TCRs, they have comparably low affinities to their antigens (1, 23–27). Thus, the dissociation constants of wild-type  $\alpha\beta$ - and  $\gamma\delta$ -TCRs are rarely below  $10^{-7}$  M (28), whereas antibodies or receptors and their ligands often show dissociation constants in the picomolar range. This makes it difficult to investigate their antigen recognition properties because many biochemical techniques rely on high affinity interactions. Although it is known that  $\gamma\delta$ -TCRs may recognize a wide variety of antigens ranging from unmodified proteins to low molecular mass ligands (1–4), the molecular details of epitope recognition are largely unknown. Even for the prominent human  $V\gamma 9V\delta 2$ -T cells, which recognize prenyl-pyrophosphates, it is still unknown how these small ligands are presented (29). So far, only few structures of  $\gamma\delta$ -TCRs have been resolved (27, 30–32), whereas the structures and antigen recognition properties of many  $\alpha\beta$ -TCR molecules are well characterized (33–36).

We used extensive site-directed mutagenesis of both the target antigen and the M88 TCR for characterizing their interaction. However, we are well aware that full structural characterization will require co-crystallization of M88 and its antigenic target. From our mutagenesis experiments, we can conclude that the target epitope of M88 is relatively “broad” because M88 recognizes different proteins and because certain non-conservative amino acid substitutions in the target antigen(s) are tolerated. Such broad recognition specificities are reminiscent of both the pattern recognition features of innate immune receptors (37) and “polyspecificity” of  $\alpha\beta$ -TCR molecules (34).

M88 recognized several functionally and structurally unrelated proteins from evolutionally very diverse species. Because the epitope is conformational rather than sequential, sequence comparison of candidate proteins would not allow prediction of their immunogenicity. It is therefore possible, or even likely,

that the epitope is present in additional, as yet undefined proteins, which also might have the capacity to activate M88. To be recognized by M88, the epitope must be exposed on the surface of the target protein. This may not be the case for all proteins carrying a compatible amino acid sequence. Therefore, only detailed structural data of the candidate proteins may allow predictions. High resolution structures are so far available for only two of the eight proteins investigated here: Ec-IF1 (21) and EcK-RS (38). Interestingly, EcK-RS expresses the sequence KTRR (amino acids 20 to 23) in a surface-exposed  $\alpha$ -helix. This is similar to the sequence KMRK at positions 39 to 42 in the  $3_{10}$   $\alpha$ -helix of EclF1 and may hint to a common recognition motif. For the other six proteins, structural data are not available or only from domains that do not contain the candidate epitope region.

The fact that the M88 epitope is present in human and microbial proteins raises the possibility of molecular mimicry (39) in the pathogenesis of  $\gamma\delta$ -TCR-mediated myositis. In retrospect, it must remain open how the break in tolerance may have occurred in the meanwhile deceased index patient, considering that the influence of the microbial environment on autoimmunity is complex (40). In the muscle tissue of the patient,  $\gamma\delta$ -T cells surrounded, invaded, and destroyed skeletal muscle fibers as demonstrated by immunohistochemistry and electron microscopy (8). An analogous type of T cell-mediated lesion occurs in other forms of myositis in which  $CD8^+$   $\alpha\beta$ -T cells invade and destroy muscle fibers in a very similar way (9, 41–45). In  $\alpha\beta$ -T cell-mediated myositis, it is assumed that the attacked muscle fibers express unknown MHC class I-bound peptides on their surface. By analogy, one may assume that a surface-exposed antigen is recognized in  $\gamma\delta$ -T cell-mediated myositis. It remains speculative whether an intracellular antigen such as AA-RS can reach the muscle surface under pathological conditions. Some targets of lupus autoantibodies are indeed accessible on the cell surface (46), and human lysyl-RS may be excreted from intact human cells after induction by TNF- $\alpha$  (47). Interestingly, several AA-RS, including histidyl-tRNA synthetase, were shown to attract lymphocytes and dendritic cells by activating CCR5 and CCR3 chemokine receptors, suggesting that AA-RS liberated from damaged myofibers might recruit immune cells that induce and perpetuate adaptive and innate immune responses in myositis (48).

Autoantibodies against nuclear or cytoplasmic antigens, including anti-AA-RS antibodies, are found in ~20% of patients with myositis (13, 14, 49). Although it is unknown whether these antibodies play a direct pathogenic role, they serve as clinical markers. Antibodies against histidyl-tRNA synthetase, also called anti-Jo-1, account for the majority of the anti-synthetase antibodies. In  $\gamma\delta$ -TCR-mediated myositis, the pathogenic  $\gamma\delta$ -T cells target the same antigen that is recognized by antibodies in other forms of myositis. Although we could block M88 recognition of histidyl-tRNA synthetase with human anti-histidyl-tRNA synthetase antibody, this does not necessarily imply that the  $\gamma\delta$ -T cell and B cell epitopes are identical. Regardless of epitope location, recognition of AA-RS by both  $\gamma\delta$ -T cells and autoantibodies reveals an intriguing link between T and B cell responses in autoimmune myositis.



## Targets of an Autoreactive Human $\gamma\delta$ -TCR

*Acknowledgments*—We thank Hartmut Wekerle for support and valuable comments, Stephan Uebel for peptide synthesis, Friedrich Lottspeich for permission to use his HPLC apparatus, Dieter Jenne and Naoto Kawakami for comments, and Elisabeth Weyher and Reinhard Mentele for expert technical assistance with circular dichroism spectroscopy and protein characterization.

### REFERENCES

- Chien, Y. H., and Konigshofer, Y. (2007) Antigen recognition by  $\gamma\delta$  T cells. *Immunol. Rev.* **215**, 46–58
- Beetz, S., Wesch, D., Marischen, L., Welte, S., Oberg, H. H., and Kabelitz, D. (2008) Innate immune functions of human  $\gamma\delta$  T cells. *Immunobiology* **213**, 173–182
- Hayday, A. C. (2009)  $\gamma\delta$  T cells and the lymphoid stress-surveillance response. *Immunity* **31**, 184–196
- Bonneville, M., O'Brien, R. L., and Born, W. K. (2010)  $\gamma\delta$  T cell effector functions: A blend of innate programming and acquired plasticity. *Nat. Rev. Immunol.* **10**, 467–478
- Wucherpfennig, K. W., Newcombe, J., Li, H., Keddy, C., Cuzner, M. L., and Hafler, D. A. (1992)  $\gamma\delta$  T-cell receptor repertoire in acute multiple sclerosis lesions. *Proc. Natl. Acad. Sci. U.S.A.* **89**, 4588–4592
- Blink, S. E., and Miller, S. D. (2009) The contribution of  $\gamma\delta$  T cells to the pathogenesis of EAE and MS. *Curr. Mol. Med.* **9**, 15–22
- Zhang, L., Jin, N., Nakayama, M., O'Brien, R. L., Eisenbarth, G. S., and Born, W. K. (2010)  $\gamma\delta$  T cell receptors confer autonomous responsiveness to the insulin-peptide B:9–23. *J. Autoimmun.* **34**, 478–484
- Hohlfeld, R., Engel, A. G., Ii, K., and Harper, M. C. (1991) Polymyositis mediated by T lymphocytes that express the  $\gamma\delta$  receptor. *N. Engl. J. Med.* **324**, 877–881
- Dalakas, M. C. (2004) Inflammatory disorders of muscle: Progress in polymyositis, dermatomyositis and inclusion body myositis. *Curr. Opin. Neurol.* **17**, 561–567
- Pluschke, G., Rüegg, D., Hohlfeld, R., and Engel, A. G. (1992) Autoaggressive myocytotoxic T lymphocytes expressing an unusual  $\gamma\delta$  T cell receptor. *J. Exp. Med.* **176**, 1785–1789
- Wiendl, H., Malotka, J., Holzwarth, B., Weltzien, H. U., Wekerle, H., Hohlfeld, R., and Dornmair, K. (2002) An autoreactive  $\gamma\delta$  TCR derived from a polymyositis lesion. *J. Immunol.* **169**, 515–521
- Dornmair, K., Schneider, C. K., Malotka, J., Dechant, G., Wiendl, H., and Hohlfeld, R. (2004) Antigen recognition properties of a V $\gamma$ 1.3V $\delta$ 2-T-cell receptor from a rare variant of polymyositis. *J. Neuroimmunol.* **152**, 168–175
- Plotz, P. H. (2003) The autoantibody repertoire: Searching for order. *Nat. Rev. Immunol.* **3**, 73–78
- Levine, S. M., Rosen, A., and Casciola-Rosen, L. A. (2003) Anti-aminoacyl tRNA synthetase immune responses: Insights into the pathogenesis of the idiopathic inflammatory myopathies. *Curr. Opin. Rheumatol.* **15**, 708–713
- Shimizu, Y., Inoue, A., Tomari, Y., Suzuki, T., Yokogawa, T., Nishikawa, K., and Ueda, T. (2001) *Nature Biotech.* **19**, 751–755
- Amor, S., Groome, N., Linington, C., Morris, M. M., Dornmair, K., Gardinier, M. V., Matthieu, J. M., and Baker, D. (1994) Identification of epitopes of myelin oligodendrocyte glycoprotein for the induction of experimental allergic encephalomyelitis in SJL and Biozzi AB/H mice. *J. Immunol.* **153**, 4349–4356
- Peterson, G. L. (1977) A simplification of the protein assay method of Lowry *et al.* which is more generally applicable. *Anal. Biochem.* **83**, 346–356
- Shevchenko, A., Wilm, M., Vorm, O., and Mann, M. (1996) Mass spectrometric sequencing of proteins silver-stained polyacrylamide gels. *Anal. Chem.* **68**, 850–858
- Blank, U., Boitel, B., Mège, D., Ermonval, M., and Acuto, O. (1993) Analysis of tetanus toxin peptide/DR recognition by human T cell receptors reconstituted into a murine T cell hybridoma. *Eur. J. Immunol.* **23**, 3057–3065
- Mao, Y., Vyas, N. K., Vyas, M. N., Chen, D. H., Ludtke, S. J., Chiu, W., and Quioco, F. A. (2004) Structure of the bifunctional and Golgi-associated formiminotransferase cyclodeaminase octamer. *EMBO J.* **23**, 2963–2971
- Sette, M., van Tilborg, P., Spurio, R., Kaptein, R., Paci, M., Gualerzi, C. O., and Boelens, R. (1997) The structure of the translational initiation factor IF1 from *E. coli* contains an oligomer-binding motif. *EMBO J.* **16**, 1436–1443
- Wang, H., Fang, Z., and Morita, C. T. (2010) V $\gamma$ 2V $\delta$ 2 T cell receptor recognition of prenyl pyrophosphates is dependent on all CDRs. *J. Immunol.* **184**, 6209–6222
- Adams, E. J., Strop, P., Shin, S., Chien, Y. H., and Garcia, K. C. (2008) An autonomous CDR3 $\delta$  is sufficient for recognition of the nonclassical MHC class I molecules T10 and T22 by  $\gamma\delta$  T cells. *Nat. Immunol.* **9**, 777–784
- Crowley, M. P., Fahrner, A. M., Baumgarth, N., Hampl, J., Gutgemann, I., Teyton, L., and Chien, Y. (2000) A population of murine  $\gamma\delta$  T cells that recognize an inducible MHC class Ib molecule. *Science* **287**, 314–316
- Shin, S., El-Diwan, R., Schaffert, S., Adams, E. J., Garcia, K. C., Pereira, P., and Chien, Y. H. (2005) Antigen recognition determinants of gd T cell receptors. *Science* **308**, 252–255
- Scotet, E., Martinez, L. O., Grant, E., Barbaras, R., Jenö, P., Guiraud, M., Monsarrat, B., Saulquin, X., Maillat, S., Estève, J. P., Lopez, F., Perret, B., Collet, X., Bonneville, M., and Champagne, E. (2005) Tumor recognition following Vg9Vd2 T cell receptor interactions with a surface F1-ATPase-related structure and apolipoprotein A-I. *Immunity* **22**, 71–80
- Xu, B., Pizarro, J. C., Holmes, M. A., McBeth, C., Groh, V., Spies, T., and Strong, R. K. (2011) Crystal structure of a gd T-cell receptor specific for the human MHC class I homolog MICA. *Proc. Natl. Acad. Sci. U.S.A.* **108**, 2414–2419
- Stone, J. D., Chervin, A. S., and Kranz, D. M. (2009) T-cell receptor binding affinities and kinetics: Impact on T-cell activity and specificity. *Immunology* **126**, 165–176
- Sarikonda, G., Wang, H., Puan, K. J., Liu, X. H., Lee, H. K., Song, Y., Distefano, M. D., Oldfield, E., Prestwich, G. D., and Morita, C. T. (2008) Photoaffinity antigens for human gd T cells. *J. Immunol.* **181**, 7738–7750
- Li, H., Lebedeva, M. I., Llera, A. S., Fields, B. A., Brenner, M. B., and Mariuzza, R. A. (1998) Structure of the V $\delta$  domain of a human gd T-cell antigen receptor. *Nature* **391**, 502–506
- Allison, T. J., Winter, C. C., Fournié, J. J., Bonneville, M., and Garboczi, D. N. (2001) Structure of a human gd T-cell antigen receptor. *Nature* **411**, 820–824
- Adams, E. J., Chien, Y. H., and Garcia, K. C. (2005) Structure of a gd T cell receptor in complex with the nonclassical MHC T22. *Science* **308**, 227–231
- Rudolph, M. G., Stanfield, R. L., and Wilson, I. A. (2006) How TCRs bind MHCs, peptides, and coreceptors. *Annu. Rev. Immunol.* **24**, 419–466
- Wucherpfennig, K. W., Allen, P. M., Celada, F., Cohen, I. R., De Boer, R., Garcia, K. C., Goldstein, B., Greenspan, R., Hafler, D., Hodgkin, P., Huseby, E. S., Krakauer, D. C., Nemazee, D., Perelson, A. S., Pinilla, C., Strong, R. K., and Sercarz, E. E. (2007) Polyspecificity of T cell and B cell receptor recognition. *Semin. Immunol.* **19**, 216–224
- Ishizuka, J., Stewart-Jones, G. B., van der Merwe, A., Bell, J. I., McMichael, A. J., and Jones, E. Y. (2008) The structural dynamics and energetics of an immunodominant T cell receptor are programmed by its V $\beta$  domain. *Immunity* **28**, 171–182
- Garcia, K. C., Adams, J. J., Feng, D., and Ely, L. K. (2009) The molecular basis of TCR germ line bias for MHC is surprisingly simple. *Nat. Immunol.* **10**, 143–147
- Iwasaki, A., and Medzhitov, R. (2010) Regulation of adaptive immunity by the innate immune system. *Science* **327**, 291–295
- Onesti, S., Desogus, G., Brevet, A., Chen, J., Plateau, P., Blanquet, S., and Brick, P. (2000) Structural studies of lysyl-tRNA synthetase: Conformational changes induced by substrate binding. *Biochemistry* **39**, 12853–12861
- Oldstone, M. B. (1987) Molecular mimicry and autoimmune disease. *Cell* **50**, 819–820
- Chervonsky, A. V. (2010) Influence of microbial environment on autoimmunity. *Nat. Immunol.* **11**, 28–35
- Arahata, K., and Engel, A. G. (1988) Monoclonal antibody analysis of mononuclear cells in myopathies. IV: Cell-mediated cytotoxicity and

- muscle fiber necrosis. *Ann. Neurol.* **23**, 168–173
42. Hohlfeld, R., and Engel, A. G. (1994) The immunobiology of muscle. *Immunol. Today* **15**, 269–274
43. Bender, A., Ernst, N., Iglesias, A., Dornmair, K., Wekerle, H., and Hohlfeld, R. (1995) T cell receptor repertoire in polymyositis: clonal expansion of autoaggressive CD8<sup>+</sup> T cells. *J. Exp. Med.* **181**, 1863–1868
44. Goebels, N., Michaelis, D., Engelhardt, M., Huber, S., Bender, A., Pongratz, D., Johnson, M. A., Wekerle, H., Tschopp, J., Jenne, D., and Hohlfeld, R. (1996) Differential expression of perforin in muscle-infiltrating T cells in polymyositis and dermatomyositis. *J. Clin. Invest.* **97**, 2905–2910
45. Seitz, S., Schneider, C. K., Malotka, J., Nong, X., Engel, A. G., Wekerle, H., Hohlfeld, R., and Dornmair, K. (2006) Reconstitution of paired T cell receptor  $\alpha$ - and  $\beta$ -chains from microdissected single cells of human inflammatory tissues. *Proc. Natl. Acad. Sci. U.S.A.* **103**, 12057–12062
46. Casciola-Rosen, L. A., Anhalt, G., and Rosen, A. (1994) Autoantigens targeted in systemic lupus erythematosus are clustered in two populations of surface structures on apoptotic keratinocytes. *J. Exp. Med.* **179**, 1317–1330
47. Park, S. G., Kim, H. J., Min, Y. H., Choi, E. C., Shin, Y. K., Park, B. J., Lee, S. W., and Kim, S. (2005) Human lysyl-tRNA synthetase is secreted to trigger proinflammatory response. *Proc. Natl. Acad. Sci. U.S.A.* **102**, 6356–6361
48. Howard, O. M., Dong, H. F., Yang, D., Raben, N., Nagaraju, K., Rosen, A., Casciola-Rosen, L., Härtlein, M., Kron, M., Yang, D., Yiadom, K., Dwivedi, S., Plotz, P. H., and Oppenheim, J. J. (2002) Histidyl-tRNA synthetase and asparaginyl-tRNA synthetase, autoantigens in myositis, activate chemokine receptors on T lymphocytes and immature dendritic cells. *J. Exp. Med.* **196**, 781–791
49. Dalakas, M. C. (2010) Immunotherapy of myositis: Issues, concerns, and future prospects. *Nat. Rev. Rheumatol.* **6**, 129–137
50. Arden, B., Clark, S. P., Kabelitz, D., and Mak, T. W. (1995) Human T-cell receptor variable gene segment families. *Immunogenetics* **42**, 455–500